

# Compact Bidirectional Transformer for Image Captioning

Yuanen Zhou<sup>1</sup>, Zhenzhen Hu<sup>1</sup>, Daqing Liu<sup>2</sup>, Huixia Ben<sup>1</sup>, Meng Wang<sup>1</sup>

<sup>1</sup>School of Computer Science and Information Engineering, Hefei University of Technology

<sup>2</sup>JD Explore Academy, JD.com Inc

{y.e.zhou.hb, huzhen.ice, liudq.ustc, eric.mengwang }@gmail.com, huixiabn@mail.hfut.edu.cn

## Abstract

Most current image captioning models typically generate captions from left to right. This unidirectional property makes them can only leverage past context but not future context. Though recent refinement-based models can exploit both past and future context by generating a new caption in the second stage based on pre-retrieved or pre-generated captions in the first stage, the decoder of these models generally consists of two networks (i.e. a retriever or captioner in the first stage and a refiner in the second stage), which can only be executed sequentially. In this paper, we introduce a Compact Bidirectional Transformer model for image captioning that can leverage bidirectional context implicitly and explicitly while the decoder can be executed parallelly. Specifically, it is implemented by tightly coupling left-to-right(L2R) and right-to-left(R2L) flows into a single compact model (i.e. implicitly) and optionally allowing interaction of the two flows(i.e. explicitly), while the final caption is chosen from either L2R or R2L flow in a sentence-level ensemble manner. We conduct extensive ablation studies on MSCOCO benchmark and find that the compact architecture, which serves as a regularization for implicitly exploiting bidirectional context, and the sentence-level ensemble play more important roles than the explicit interaction mechanism. By combining with word-level ensemble seamlessly, the effect of sentence-level ensemble is further enlarged. We further extend the conventional one-flow self-critical training to the two-flows version under this architecture and achieve new state-of-the-art results in comparison with non-vision-language-pretraining models. Source code is available at <https://github.com/YuanEZHou/CBTrans>.

## INTRODUCTION

Image captioning (Vinyals et al. 2015; Yang et al. 2019; Pan et al. 2020; Zhou et al. 2021), which aims at describing the visual content of an image with natural language sentences, is one of the important tasks to connect vision and language. Inspired by the sequence-to-sequence model (Sutskever, Vinyals, and Le 2014) for neural machine translation, most proposed models typically follow the encoder/decoder paradigm. In between, a convolutional neural network (CNN) or Transformer is utilized to encode an input image and recurrent neural networks (RNN) or Transformer (Vaswani et al. 2017) is adopted as sentence decoder to generate a caption.

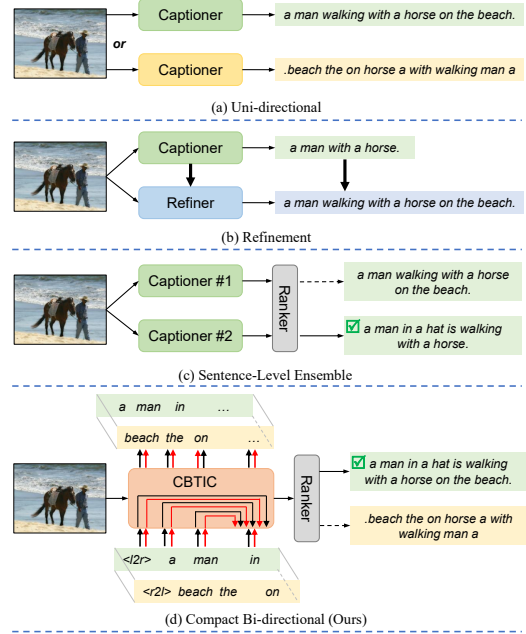


Figure 1: A conceptual overview of (a) Uni-directional generation, including left-to-right(L2R) and right-to-left(R2L), (b) Refinement-based generation, (c) Sentence-Level Ensemble and (d) our proposed Compact Bidirectional Transformer for Image Captioning (CBTIC), which combines the advantage of (abc), where L2R and R2L ‘flows’ share a unified network and interaction between the two ‘flows’ is optionally allowed inside.

Most current image captioning models (Pan et al. 2020; Zhang et al. 2021b) typically adopt the left-to-right generation manner(as shown in Figure 1(a)), which is straightforward. During training and testing, they can only access the past context for the current prediction. This unidirectional property can’t make them exploit bidirectional context for better decoding.

To make use of bidirectional context during decoding, refinement-based methods (Sammani and Elsayed 2019; Sammani and Melas-Kyriazi 2020; Wang et al. 2020; Song et al. 2021; Zhang et al. 2021c) are proposed recently. The

decoder of this type of models typically consists of two networks (as shown in Figure 1(b)). The first network is usually a primary captioner or an image-text retriever, which is used to generate or retrieve a related sentence. After that, a senior refiner, which is the second caption network, generates the final caption by being allowed to attend to the sentence produced before. This semantic attention can help the senior refiner to look at both past and future semantic context and thus improve decoding at every time step. However, the two networks in the decoder can only be executed sequentially, which can not make full use of the parallelizability of GPU device.

In this work, we introduce a Compact Bidirectional Transformer model for image captioning (dubbed as CBTIC) that can leverage bidirectional context implicitly and explicitly while the decoder can be executed parallelly. Specifically, it is implemented by tightly coupling the L2R and the R2L flows into a single compact model and optionally allowing interaction between the two flows (as shown in Figure 1(d)). The parallelism of our decoder is obvious since it is composed of a single Transformer decoder. We claim our decoder can exploit bidirectional context explicitly since we optionally allow interaction between L2R and R2L flows and implicitly since one copy of shared parameters has the ability of supporting both L2R and R2L decoding. Let’s take Figure 1(d) as an example. During training, each image is associated with two captions instead of one caption as in the conventional L2R captioning models. One caption is from left to right with a  $\langle l2r \rangle$  prefix and the other one is from right to left with a  $\langle r2l \rangle$  prefix. Inside the CBTIC model, the generation of a target word (e.g., ‘walking’) can not only depend on previous words in its own flow (e.g., ‘a man in a hat is’, i.e., past context) but also optionally previous words in the other flow (e.g., ‘beach the on horse a with’, i.e., future context). The joint loss is composed of both L2R and R2L losses and the model is end-to-end trainable. During inference, CBTIC model takes both  $\langle l2r \rangle$  and  $\langle r2l \rangle$  as the text input in the first step and optionally allows interaction between the two flows along the entire decoding process. Finally, the output caption of L2R ‘flow’ and the one of R2L ‘flow’ are ranked based on their probabilities and the larger one is chosen as the output (i.e. sentence-level ensemble).

We conduct extensive ablation studies on the MSCOCO benchmark dataset to better understand and verify the effectiveness of this model. The **compact** architecture serves as a good regularization for **implicitly** exploiting bidirectional context and a single CBTIC model achieves an effect of **sentence-level ensemble**, which usually needs to train and save two models for improving final predictions as shown in Figure 1(c). By combining with word-level ensemble, the effect of sentence-level ensemble is further enlarged. Overall, the compact bidirectional architecture and sentence-level ensemble play more important roles than the **explicit** interaction mechanism. Finally, we further extend the conventional one-flow self-critical training to the two-flows version under this model architecture and achieve new state-of-the-art results in comparison with non-vision-language-pretraining models.

The main contributions are summarized as follows:

- We introduce a Compact Bidirectional Transformer model for image captioning that can leverage bidirectional context implicitly and explicitly while the decoder is parameter-efficient and can be executed parallelly. And we conduct extensive ablation studies to better understand this architecture.
- We further propose to combine word-level and sentence-level ensemble seamlessly and extend the conventional one-flow self-critical training to the two-flows version under this architecture and achieve new state-of-the-art results in comparison with non-vision-language-pretraining models.

## RELATED WORK

### Image Captioning

Over the last few years, a broad collection of methods have been proposed in the field of image captioning. In a nutshell, we have gone through grid-feature (Xu et al. 2015; Jiang et al. 2020) then region-feature (Anderson et al. 2018) and relation-aware visual feature (Yao et al. 2018; Yang et al. 2019) on the image encoding side. On the sentence decoding side, we have witnessed LSTM (Vinyals et al. 2015), CNN (Gu et al. 2017) and Transformer (Cornia et al. 2020) equipped with various attention (Huang et al. 2019; Zhou et al. 2020b; Pan et al. 2020) as the decoder. On the training side, models are typically trained by cross-entropy loss and then Reinforcement Learning (Rennie et al. 2017), which enables the use of non-differentiable caption metrics as optimization objectives and makes a notable achievement. Recently, vision-language pre-training has also been adopted for image captioning and shows remarkable results. These models (Zhou et al. 2020a; Li et al. 2020; Zhang et al. 2021a) are firstly pre-trained on large image-text corpus and then finetuned. Though impressive performance has been achieved, most state-of-the-art models adopt the left-to-right generation manner, which is straightforward but can’t exploit future context. To make use of bidirectional context as far as possible, refinement-based methods are proposed recently, where (Sammani and Elsayed 2019; Sammani and Melas-Kyriazi 2020; Song et al. 2021) generate a primary caption and (Wang et al. 2020; Zhang et al. 2021c) retrieve a related primary caption in the first stage and both them generate a senior caption in the second stage. There is also an early work (Wang et al. 2016) that tries to overcome the shortcomings of unidirectional model by combining the output captions of two separate forward and backward LSTM networks. Different from these models, CBTIC is a single Compact Bidirectional Transformer model.

### Multi-task Learning

Multi-task learning is a useful learning paradigm to improve the supervision and the generalization performance of a task by jointly training it with related tasks (Caruana 1997). Here, we only review some multi-task learning works related to captioning. To the best of our knowledge, there are roughly two types so far. One is to jointly train the task of captioning and syntax generation (e.g. Part-of-Speech) (Zhao et al. 2018; Deshpande et al. 2019; Wang et al. 2019a; Hou

et al. 2019). The other one is to train a unified captioning model on multilingual (e.g. English and Chinese ) captioning datasets (Elliott, Frank, and Hasler 2015; Wang et al. 2019b). Different from the above multi-task learning models, one task is the L2R generation and the other one is the R2L generation in our CBTIC model.

## Neural Machine Translation

Neural Machine Translation (NMT) has an important impact on the research of captioning task. The standard encoder-decoder paradigm is derived from NMT (Sutskever, Vinyals, and Le 2014; Bahdanau, Cho, and Bengio 2014). A complete review is beyond the scope of this paper and we only focus on works related to endow decoder with bidirectional ability. (Zhang et al. 2019) trained a backward decoder jointly with a forward decoder by matching their output probabilities to iteratively improve each other. (Chen et al. 2020) proposed to further encourage conventional autoregressive decoder to plan ahead by distilling bidirectional knowledge learned in BERT (Devlin et al. 2018). (Zhang et al. 2018) proposed asynchronous bidirectional decoding for NMT by equipping the conventional attentional forward decoder with an auxiliary backward decoder. (Zhou, Zhang, and Zong 2019) proposed a synchronous bidirectional neural machine translation that predicts its outputs using left-to-right and right-to-left decoding simultaneously and interactively. This work pursues the spirit of (Zhou, Zhang, and Zong 2019) for image captioning and we find that it is the compact architecture and sentence-level ensemble mechanism instead of explicit interaction that contributes more to the model. This is overlooked in (Zhou, Zhang, and Zong 2019) and indicates that explicit interaction is overestimated. What’s more, we further propose to combine word-level and sentence-level ensemble seamlessly and extend the conventional one-flow self-critical training to the two-flows version under this architecture.

## Approach

In this section, we first present the architecture of our CBTIC model built on the well-known Transformer (Vaswani et al. 2017) and then introduce the training procedure for model optimization.

### CBTIC Model

Firstly, a pre-trained object detector (Ren et al. 2015) represents an image  $I$  as a set of region features. Then given the image region features, CBTIC aims to take advantage of bidirectional property in a single model to generate a sensible caption. The architecture of CBTIC model is illustrated in Figure 2, which consists of an encoder and decoder.

**Image Features Encoder.** The encoder, which is basically the same as the Transformer encoder (Vaswani et al. 2017), takes the image region features as inputs and outputs the contextual region features. It consists of a stack of  $L$  identical layers. Each layer has two sublayers. The first is a multi-head self-attention sublayer and the second is a

position-wise feed-forward sublayer. Both sublayers are followed by residual connection (He et al. 2016) and layer normalization (Ba, Kiros, and Hinton 2016) operations for stable training. Multi-head self-attention builds on the scaled dot-product attention, which operates on a query  $Q$ , key  $K$  and value  $V$  as:

$$Attention(Q, K, V) = softmax(\frac{QK^T}{\sqrt{d_k}})V, \quad (1)$$

where  $d_k$  is the dimension of the key. Multi-head self-attention firstly projects the queries, keys and values  $h$  times with different learned linear projections and then computes scaled dot-product attention for each one. After that, it concatenates the results and projects them with another learned linear projection:

$$H_i = Attention(QW_i^Q, KW_i^K, VW_i^V), \quad (2)$$

$$MultiHead(Q, K, V) = Concat(H_1, \dots H_h)W^O, \quad (3)$$

where  $W_i^Q, W_i^K \in \mathbb{R}^{d_{model} \times d_k}$ ,  $W_i^V \in \mathbb{R}^{d_{model} \times d_v}$  and  $W^O \in \mathbb{R}^{hd_v \times d_{model}}$ . The self-attention in the encoder performs attention over itself, i.e., ( $Q = K = V$ ), which is the image region features in the first layer. After a multi-head self-attention sublayer, the position-wise feed-forward sublayer (FFN) is applied to each position separately and identically:

$$FFN(x) = max(0, xW_1 + b_1)W_2 + b_2, \quad (4)$$

where  $W_1 \in \mathbb{R}^{d_{model} \times d_{ff}}$ ,  $W_2 \in \mathbb{R}^{d_{ff} \times d_{model}}$ ,  $b_1 \in \mathbb{R}^{d_{ff}}$  and  $b_2 \in \mathbb{R}^{d_{model}}$  are learnable parameter matrices.

**Captioning Decoder.** The decoder takes contextual region features and a pair of L2R and R2L word sequences of each image as input and outputs a pair of predicted words probability sequences. To make use of order information, position encodings (Vaswani et al. 2017) are added to word embedding features. It is worth emphasizing that the L2R and R2L flows in the decoder run in parallel and the bidirectional interactive only optionally happens in the mask multi-head bidirectional interactive attention sublayer. Specifically, the decoder consists of  $L$  identical layers and each layer has three sublayers: a masked multi-head bidirectional interactive attention sublayer, a multi-head cross-attention sublayer and a position-wise feed-forward sublayer. Residual connection and layer normalization are also applied after each sublayer. The multi-head cross-attention is similar to the multi-head self-attention mentioned above except that the key and value are now contextual region features and the query is the output of its previous sublayer. The masked multi-head bidirectional interactive attention sublayer can be seen as an extension of the masked multi-head attention sublayer in the original Transformer decoder (Vaswani et al. 2017). The main difference between them lies in the scaled dot-product attention module. An intuitional illustration is shown in the right of Figure 2. Formally, the scaled dot-product attention for each head  $i$  in the original masked multi-head attention

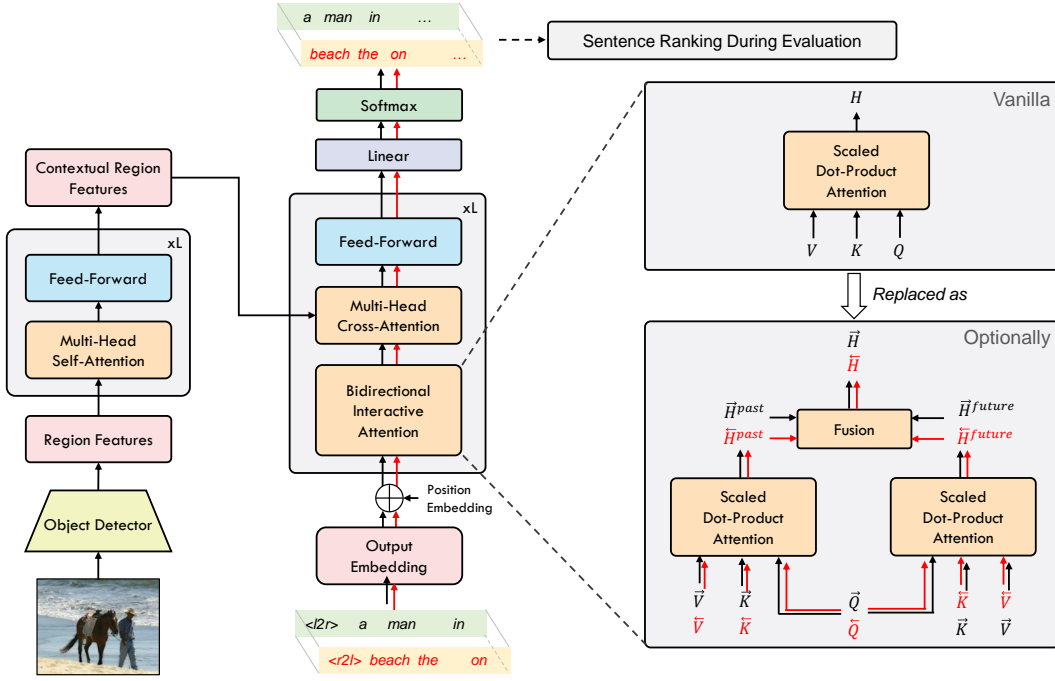


Figure 2: Illustration of Compact Bidirectional Transformer for Image Captioning (CBTIC). CBTIC model composes of an encoder (in the left) and a decoder (in the middle). An intuitional illustration of extension of the standard Scaled Dot-Product Attention module is shown on the right. Notice that the Residual Connections, Layer Normalization are omitted. The subscript of head  $i$  in Q/K/V/H is omitted for brevity. Right-to-right (R2L) flow is marked in red. Best view in color.

module is extended to:

$$\begin{aligned}
 \vec{H}_i^{past} &= \text{Attention}(\vec{Q}_i, \vec{K}_i, \vec{V}_i) \\
 \vec{H}_i^{future} &= \text{Attention}(\vec{Q}_i, \overleftarrow{K}_i, \overleftarrow{V}_i), \\
 \vec{H}_i &= \vec{H}_i^{past} + \lambda * AF(\vec{H}_i^{future})
 \end{aligned} \quad (5)$$

where  $\vec{H}_i^{past}$  is the conventional one to capture past context and  $\vec{H}_i^{future}$  is the extended part to capture future context by using query in the L2R direction and key/value in R2L direction.  $\vec{H}_i$  is the bidirectional-aware state of L2R direction by non-linearly fusing past and future context and AF denotes activation function, such as Relu or Tanh. It is worth noting that the self-attention in the decoder usually is equipped with a lower triangular matrix mask for preventing positions from attending to subsequent positions and we omit it here for brevity. And the bidirectional-aware state of R2L direction  $\overleftarrow{H}_i$  can be symmetrically computed as:

$$\overleftarrow{H}_i = \text{Attention}(\overleftarrow{Q}_i, \overleftarrow{K}_i, \overleftarrow{V}_i) + \lambda * AF(\text{Attention}(\overleftarrow{Q}_i, \vec{K}_i, \vec{V}_i)). \quad (6)$$

In particular, the masked multi-head bidirectional interactive attention sublayer degrades to the original masked multi-head attention sublayer when  $\lambda = 0$ . Finally, we use a learned linear transformation and softmax function to convert the decoder output to a pair of predicted next-token probabilities  $p(\vec{y}_t | \vec{y}_{<t}, \overleftarrow{y}_{<t}, I; \theta)$  and  $p(\overleftarrow{y}_t | \overleftarrow{y}_{<t}, \vec{y}_{<t}, I; \theta)$ , where  $\vec{y}_{<t}$  ( $\overleftarrow{y}_{<t}$ ) denotes the words sequence of L2R (R2L) direction before the  $t$ -th word of target  $\vec{y}$  ( $\overleftarrow{y}$ ) and  $\theta$  is the shared parameters.

## Training

The whole training procedure includes two stages. At the first training stage, given a triple  $(I, \vec{y}, \overleftarrow{y})$ , we pad the two sentences to equal length  $T$  without loss of generality, i.e.,  $\vec{y} = (\vec{y}_1, \vec{y}_2, \dots, \vec{y}_T)$  and  $\overleftarrow{y} = (\overleftarrow{y}_1, \overleftarrow{y}_2, \dots, \overleftarrow{y}_T)$ . We optimize the model by minimizing joint cross-entropy (XE) loss, which is composed of a L2R and R2L XE loss:

$$\begin{aligned}
 L_{XE}(\theta) &= - \sum_{t=1}^T \{ \log p(\vec{y}_t | \vec{y}_{<t}, \overleftarrow{y}_{<t}, I; \theta) \\
 &\quad + \log p(\overleftarrow{y}_t | \overleftarrow{y}_{<t}, \vec{y}_{<t}, I; \theta) \}. \quad (7)
 \end{aligned}$$

In order to prevent the bidirectional model from learning to directly generate the second half of L2R flow by copying the first half of R2L flow and vice versa,  $\overleftarrow{y}$  is chosen from the rest caption annotations of the same image (each image is annotated with five captions in the dataset) and then reversed and paired with  $\vec{y}$ .

At the second training stage, we jointly finetune the model using self-critical training (SC) (Rennie et al. 2017) for both L2R and R2L directions and the gradient can be expressed as:

$$\begin{aligned}
 \nabla_{\theta} L_{SC}(\theta) &= - \frac{1}{N} \sum_{n=1}^N \{ (R(\vec{y}^n) - \vec{b}) \nabla_{\theta} \log p(\vec{y}^n | I; \theta) \\
 &\quad + (R(\overleftarrow{y}^n) - \overleftarrow{b}) \nabla_{\theta} \log p(\overleftarrow{y}^n | I; \theta) \}, \quad (8)
 \end{aligned}$$

where  $R$  is the CIDEr (Vedantam, Lawrence Zitnick, and

	Cross-Entropy Loss								CIDEr Score Optimization							
	B@1	B@2	B@3	B@4	M	R	C	S	B@1	B@2	B@3	B@4	M	R	C	S
LSTM (Vinyals et al. 2015)	-	-	-	29.6	25.2	52.6	94.0	-	-	-	-	31.9	25.5	54.3	106.3	-
SCST (Rennie et al. 2017)	-	-	-	30.0	25.9	53.4	99.4	-	-	-	-	34.2	26.7	55.7	114.0	-
LSTM-A (Yao et al. 2017)	75.4	-	-	35.2	26.9	55.8	108.8	20.0	78.6	-	-	35.5	27.3	56.8	118.3	20.8
RFNet (Jiang et al. 2018)	76.4	60.4	46.6	35.8	27.4	56.5	112.5	20.5	79.1	63.1	48.4	36.5	27.7	57.3	121.9	21.2
Up-Down (Anderson et al. 2018)	77.2	-	-	36.2	27.0	56.4	113.5	20.3	79.8	-	-	36.3	27.7	56.9	120.1	21.4
GCN-LSTM (Yao et al. 2018)	77.3	-	-	36.8	27.9	57.0	116.3	20.9	80.5	-	-	38.2	28.5	58.3	127.6	22.0
LBPF (Qin et al. 2019)	77.8	-	-	37.4	28.1	57.5	116.4	21.2	80.5	-	-	38.3	28.5	58.4	127.6	22.0
SGAE (Yang et al. 2019)	77.6	-	-	36.9	27.7	57.2	116.7	20.9	80.8	-	-	38.4	28.4	58.6	127.8	22.1
AoANet (Huang et al. 2019)	77.4	-	-	37.2	28.4	57.5	119.8	21.3	80.2	-	-	38.9	29.2	58.8	129.8	22.4
X-LAN (Pan et al. 2020)	<b>78.0</b>	<b>62.3</b>	<b>48.9</b>	<b>38.2</b>	28.8	58.0	122.0	21.9	80.8	65.6	51.4	39.5	29.5	59.2	132.0	23.4
$M^2$ T (Cornia et al. 2020)	-	-	-	-	-	-	-	-	80.8	-	-	39.1	29.2	58.6	131.2	22.6
X-Transformer (Pan et al. 2020)	77.3	61.5	47.8	37.0	28.7	57.5	120.0	21.8	80.9	65.8	51.5	39.7	29.5	59.1	132.8	23.4
RSTNet (Zhang et al. 2021b)	-	-	-	-	-	-	-	-	<b>81.8</b>	-	-	<b>40.1</b>	29.8	<b>59.5</b>	135.6	23.3
CBTIC	<b>78.0</b>	62.2	48.5	37.5	<b>29.1</b>	<b>58.2</b>	<b>122.6</b>	<b>22.3</b>	81.4	<b>66.5</b>	<b>51.9</b>	39.6	<b>29.9</b>	59.1	<b>136.9</b>	<b>24.0</b>
<b>Ensemble</b>																
SCST (Rennie et al. 2017) $\Sigma$	-	-	-	32.8	26.7	55.1	106.5	-	-	-	-	35.4	27.1	56.6	117.5	-
RFNet (Jiang et al. 2018) $\Sigma$	77.4	61.6	47.9	37.0	27.9	57.3	116.3	20.8	80.4	64.7	50.0	37.9	28.3	58.3	125.7	21.7
GCN-LSTM (Yao et al. 2018) $\Sigma$	77.4	-	-	37.1	28.1	57.2	117.1	21.1	80.9	-	-	38.3	28.6	58.5	128.7	22.1
SGAE (Yang et al. 2019) $\Sigma$	-	-	-	-	-	-	-	-	81.0	-	-	39.0	28.4	58.9	129.1	22.2
HIP (Yao et al. 2019) $\Sigma$	-	-	-	38.0	28.6	57.8	120.3	21.4	-	-	-	39.1	28.9	59.2	130.6	22.3
AoANet (Huang et al. 2019) $\Sigma$	78.7	-	-	38.1	28.5	58.2	122.7	21.7	81.6	-	-	40.2	29.3	59.4	132.0	22.8
$M^2$ T (Cornia et al. 2020) $\Sigma$	-	-	-	-	-	-	-	-	82.0	-	-	40.5	29.7	59.5	134.5	23.5
X-LAN (Pan et al. 2020) $\Sigma$	78.8	63.4	49.9	39.1	29.1	58.5	124.5	22.2	81.6	66.6	52.3	40.3	29.8	59.6	133.7	23.6
X-Transformer (Pan et al. 2020) $\Sigma$	77.8	62.1	48.6	37.7	29.0	58.0	122.1	21.9	81.7	66.8	52.6	40.7	29.9	59.7	135.3	23.8
CBTIC	<b>79.1</b>	<b>63.9</b>	<b>50.3</b>	<b>39.4</b>	<b>29.8</b>	<b>59.3</b>	<b>127.8</b>	<b>23.1</b>	<b>82.7</b>	<b>67.9</b>	<b>53.5</b>	<b>41.1</b>	<b>30.4</b>	<b>60.1</b>	<b>140.3</b>	<b>24.3</b>

Table 1: Performance comparisons on MSCOCO Karpathy test split, where B@N, M, R, C and S are short for BLEU@N, METEOR, ROUGE-L, CIDEr and SPICE scores. All values are reported as percentage (%).  $\Sigma$  indicates model ensemble.

Parikh 2015) score function, and  $b$  is the baseline score. We adopt the baseline score proposed in (Luo 2020), where the baseline score is defined as the average reward of the rest samples rather than the original greedy decoding reward. We sample  $N = 5$  captions for each image and each direction and  $\vec{y}^n$  ( $\overleftarrow{y}^n$ ) is the  $n$ -th sampled caption of L2R (R2L) direction.

## EXPERIMENTS

### Dataset and Evaluation Metrics.

MSCOCO (Chen et al. 2015) is the widely used benchmark for image captioning. We use the ‘Karpathy’ splits (Karpathy and Fei-Fei 2015) for offline experiments. This split contains 113, 287 training images, 5, 000 validation images and 5, 000 testing images. Each image has 5 captions. We also upload generated captions of MSCOCO official testing set, which contains 40, 775 images for online evaluation. The quality of captions is evaluated by standard metrics (Chen et al. 2015), including BLEU-1/4 (Papineni et al. 2002), METEOR (Banerjee and Lavie 2005), ROUGE (Lin 2004), SPICE (Anderson et al. 2016), and CIDEr (Vedantam, Lawrence Zitnick, and Parikh 2015), denoted as B1/4, M, R, S, and C for short.

### Implementation Details.

Each image is represented as a set of region features with 2, 048 dimensions extracted by object detector (Ren et al. 2015). We try two kinds of features, i.e., Up-Down feature

Metrics \ $\lambda$	0.0		0.1		0.4	
	B@1	C	B@1	C	B@1	C
Up-Down Feat.						
Tanh	76.5	114.2	76.5	114.0	76.8	114.4
ReLU	76.5	114.2	<b>76.9</b>	<b>115.0</b>	76.6	114.4
VinVL Feat.						
ReLU	78.1	121.6	<b>78.5</b>	<b>122.4</b>	78.3	121.5

Table 2: Performance on MSCOCO validation set with different activation functions and  $\lambda$ . Beam size is set to 1.

with 36 regions per image (Anderson et al. 2018), and VinVL feature with up to 50 regions per image (Zhang et al. 2021a), which is extracted by a more powerful detector. The dictionary is built by dropping the words that occur less than 5 times and ends up with a vocabulary of 9, 487. Captions longer than 16 words are truncated. Our CBTIC model almost follows the same model hyper-parameters setting as in (Vaswani et al. 2017) ( $d_{model} = 512$ ,  $d_k = d_v = 64$ ,  $d_{ff} = 2048$ ,  $L = 6$ ,  $h = 8$ ,  $p_{dropout} = 0.1$ ). As for the training process, we train CBTIC under cross-entropy loss for 15 epochs with a mini batch size of 10, and optimizer in (Vaswani et al. 2017) is used with a learning rate initialized by  $5e-4$  and the warmup step is set to 20000. We increase the scheduled sampling probability by 0.05 every 5 epochs. We then optimize the CIDEr score with self-critical training for another 15 epochs with an initial learning rate of  $1e-5$ .

Model	BLEU-1		BLEU-2		BLEU-3		BLEU-4		METEOR		ROUGE		CIDEr	
	c5	c40	c5	c40										
SCST (Rennie et al. 2017)	78.1	93.7	61.9	86.0	47.0	75.9	35.2	64.5	27.0	35.5	56.3	70.7	114.7	116.7
Up-Down (Anderson et al. 2018)	80.2	95.2	64.1	88.8	49.1	79.4	36.9	68.5	27.6	36.7	57.1	72.4	117.9	120.5
RFNet (Jiang et al. 2018)	80.4	95.0	64.9	89.3	50.1	80.1	38.0	69.2	28.2	37.2	58.2	73.1	122.9	125.1
GCN-LSTM (Yao et al. 2018)	80.8	95.9	65.5	89.3	50.8	80.3	38.7	69.7	28.5	37.6	58.5	73.4	125.3	126.5
SGAE (Yang et al. 2019)	81.0	95.3	65.6	89.5	50.7	80.4	38.5	69.7	28.2	37.2	58.6	73.6	123.8	126.5
ETA (Li et al. 2019)	81.2	95.0	65.5	89.0	50.9	80.4	38.9	70.2	28.6	38.0	58.6	73.9	122.1	124.4
AoANet (Huang et al. 2019)	81.0	95.0	65.8	89.6	51.4	81.3	39.4	71.2	29.1	38.5	58.9	74.5	126.9	129.6
GCN-LSTM+HIP (Yao et al. 2019)	81.6	95.9	66.2	90.4	51.5	81.6	39.3	71.0	28.8	38.1	59.0	74.1	127.9	130.2
$M^2$ T (Cornia et al. 2020)	81.6	96.0	66.4	90.8	51.8	82.7	39.7	72.8	29.4	39.0	59.2	74.8	129.3	132.1
X-Transformer(Pan et al. 2020)	81.9	95.7	66.9	90.5	52.4	82.5	40.3	72.4	29.6	39.2	59.5	75.0	131.1	133.5
GET (Ji et al. 2021)	81.6	96.1	66.5	90.9	51.9	82.8	39.7	72.9	29.4	38.8	59.1	74.4	130.3	132.5
RSTNet (Zhang et al. 2021b)	82.1	96.4	67.0	91.3	52.2	83.0	40.0	73.1	29.6	39.1	59.5	74.6	131.9	134.0
<b>CBTIC</b>	<b>82.3</b>	<b>96.5</b>	<b>67.5</b>	<b>91.8</b>	<b>52.8</b>	<b>83.7</b>	<b>40.5</b>	<b>73.5</b>	<b>30.0</b>	<b>39.6</b>	<b>59.6</b>	<b>75.0</b>	<b>135.0</b>	<b>138.6</b>

Table 3: Leaderboard of the published state-of-the-art image captioning models on the MSCOCO online testing server, where B@N, M, R, and C are short for BLEU@N, METEOR, ROUGE-L, and CIDEr scores. All values are reported as percentage (%).

During testing, unless stated otherwise, we use the standard beam search for conventional Transformer model with beam size 3, which is the best width based on our observation. It is worth noting that the beam search method for CBTIC model is a little different from the standard one. Specifically, if the total beam size is 4, then both L2R and R2L flow should independently keep a standard beam search with beam size 2 for each step. Unless stated otherwise, the beam size of each flow is set to 2 for CBTIC model.

## Quantitative Results

In this section, we will quantitatively analyze CBTIC model in detail by answering the following questions.

**What is the effect of Fusion function with different  $\lambda$ ?** Following previous practice (Zhou, Zhang, and Zong 2019), we choose to use the simple non-linear fusion mechanism. From Table 2, we can find that the explicit interaction mechanism only improves slightly over the baseline ( $\lambda = 0$ ) when proper  $\lambda = 0.1$  is selected. This indicates that the explicit interaction mechanism is not the main contributor of this model, which is different from (Zhou, Zhang, and Zong 2019), and motivates us to further decipher this architecture. In the following, we select ReLU and set  $\lambda = 0.1$  as default, unless stated otherwise.

**What is the effect of each component that constitutes the CBTIC model?** To further investigate the effectiveness of CBTIC model and each component, we conduct substantial ablation studies, as shown in Table 4. Before diving into the details, we emphasize that CBTIC model doesn't increase any model parameters except two special symbols (i.e.,  $\langle l2r \rangle$  and  $\langle r2l \rangle$ ) embedding compared to the standard baseline model and they share the same training script.

Firstly, by comparing the 9th row with the 1st and 5th rows, we can find that the whole CBTIC model outperforms Transformer(L2R) and Transformer(R2L) models more than 2.7% in CIDEr metric. And the advantage of our CBTIC model is more obvious when using better VinVL feature by comparing the 18th row with the 10th row (e.g., more than

#	Metrics Models	Cross-Entropy Loss			
		B@4	M	R	C
Up-Down Feat.					
1	Transformer(L2R)	35.4	27.8	56.3	111.7
2	Transformer(L2R-seed1)	35.4	27.7	56.3	112.3
3	Sentence-Level Ensemble	35.1	28.1	56.4	112.5
4	Transformer(L2R)	35.4	27.8	56.3	111.7
5	Transformer(R2L)	33.9	27.1	55.2	109.6
6	Sentence-Level Ensemble	34.6	27.8	56.0	111.7
7	CBTIC(only keep R2L during eval.)	34.3	27.5	56.0	112.6
8	CBTIC(only keep L2R during eval.)	<b>35.7</b>	27.7	56.7	113.4
9	CBTIC	35.6	<b>28.1</b>	<b>56.8</b>	<b>114.4</b>
VinVL Feat.					
10	Transformer(L2R)	37.1	28.4	57.3	117.6
11	Transformer(L2R-seed1)	36.6	28.6	57.2	117.3
12	Sentence-Level Ensemble	36.8	28.8	57.4	118.5
13	Transformer(L2R)	37.1	28.4	57.3	117.6
14	Transformer(R2L)	35.5	28.1	56.9	117.0
15	Sentence-Level Ensemble	37.1	29.0	57.9	119.9
16	CBTIC(only keep R2L during eval.)	36.1	28.4	57.3	119.4
17	CBTIC(only keep L2R during eval.)	37.8	28.9	58.0	121.3
18	CBTIC	<b>37.8</b>	<b>29.1</b>	<b>58.2</b>	<b>121.8</b>

Table 4: Ablation studies on MSCOCO validation set. The default random seed is 0.

4.2% gain in CIDEr metric). This proves the overall effectiveness of CBTIC model.

Secondly, by comparing the 7th/8th row with the 5th/1st row, we can find that the **compact** architecture of CBTIC model can serve as a good regularization by improving the performance from 109.6/111.7 CIDEr to 112.6/113.4 CIDEr. And we can also see similar trend when using better VinVL feature by comparing the 16th/17th row with the 14th/13th row.

Thirdly, we investigate the effect of sentence-level ensemble, which is a natural part of our CBTIC model since we have to choose one final caption from the outputs of L2R and R2L 'flows'. By comparing the 9th row with the 8th

Cross-Entropy Loss		CIDEr Score Optimization	
Good Cases		Better Feature Effect	Bad Cases
 <p>Image_id:462565</p> <p><b>Transformer(l2r):</b> a man riding a bike down a street next to a tall building.  <b>Transformer(r2l):</b> a group of people riding bikes down a city street.  <b>CBTIC:</b> a group of people riding bikes down a city street.  <b>CBTIC(VinVL-feat):</b> a group of people riding bikes down a street.  <b>GT:</b> a group of bicyclists are riding in the bike lane.</p>	 <p>Image_id:489023</p> <p><b>Transformer(l2r):</b> a man standing on a field with a soccer ball.  <b>Transformer(r2l):</b> a group of people playing with a soccer ball on a field.  <b>CBTIC:</b> a group of people playing soccer on a field.  <b>CBTIC(VinVL-feat):</b> a group of men playing soccer on a field.  <b>GT:</b> some men are playing soccer on a field with a blue ball.</p>	 <p>Image_id:310391</p> <p><b>Transformer(l2r):</b> a blue car parked on the grass with a UNK.  <b>Transformer(r2l):</b> of an old truck with a UNK on top of it.  <b>CBTIC:</b> a blue car parked in the grass with a UNK.  <b>CBTIC(VinVL-feat):</b> an old blue car with a surfboard on top of it.  <b>GT:</b> an old car with surfboards on the top.</p>	 <p>Image_id:309120</p> <p><b>Transformer(l2r):</b> a man standing on a field with a soccer ball.  <b>Transformer(r2l):</b> of a man with a soccer ball on a field.  <b>CBTIC:</b> of a man with a soccer ball on a field.  <b>CBTIC(VinVL-feat):</b> a man holding a soccer ball on a field.  <b>GT:</b> the soccer player is bringing back the ball into play.</p>
 <p>Image_id:394240</p> <p><b>Transformer(l2r):</b> a row of motorcycles parked on a street.  <b>Transformer(r2l):</b> two motorcycles are parked outside of a building.  <b>CBTIC:</b> a row of motorcycles parked in front of a building.  <b>CBTIC(VinVL-feat):</b> a row of parked motorcycles sitting on the side of a street.  <b>GT:</b> a row of motorcycles parked in front of a building.</p>	 <p>Image_id:136501</p> <p><b>Transformer(l2r):</b> a baseball player is on a field with a ball.  <b>Transformer(r2l):</b> on top of a baseball player standing on a field.  <b>CBTIC:</b> a baseball player standing on a field with a ball.  <b>CBTIC(VinVL-feat):</b> of a baseball player throwing a ball on a field.  <b>GT:</b> a baseball player prepares to throw the ball.</p>	 <p>Image_id:550529</p> <p><b>Transformer(l2r):</b> a motorcycle parked on top of a wooden table.  <b>Transformer(r2l):</b> of a motorcycle parked next to a shelf.  <b>CBTIC:</b> a motorcycle parked on top of a wooden shelf.  <b>CBTIC(VinVL-feat):</b> a motorcycle parked in front of a bar of wine bottles.  <b>GT:</b> a motorbike sitting in front of a wine display case.</p>	 <p>Image_id:503311</p> <p><b>Transformer(l2r):</b> a man standing on a beach flying a kite.  <b>Transformer(r2l):</b> a person is flying a kite on the beach.  <b>CBTIC:</b> of a man flying a kite on the beach.  <b>CBTIC(VinVL-feat):</b> of a man walking on the beach flying a kite.  <b>GT:</b> a man flying a kite over a sandy beach.</p>

Figure 3: Examples of captions generated by our CBTIC model, conventional unidirectional Transformer model and human-annotated ground truth. The bad words are marked in red.

Models	Metrics	Cross-Entropy Loss			
		B@4	M	R	C
CBTIC*2		38.3	29.4	58.9	125.3
CBTIC(only keep L2R during eval.)*2		37.4	28.9	58.3	122.5
CBTIC*3		39.2	29.7	59.2	127.4
CBTIC(only keep L2R during eval.)*3		38.3	29.3	58.8	125.1
CBTIC*4		39.1	29.7	59.3	127.6
CBTIC(only keep L2R during eval.)*4		38.6	29.3	59.0	125.5

Table 5: The effect of combining model ensemble and sentence-level ensemble on MSCOCO validation set. ‘\*2’ indicates we average the word-level output probability distributions of two independently trained instances with different parameter initialization. Beam size is set to 1 and VinVL feature is used.

row, we can see the effect of sentence-level ensemble mechanism by improving the METEOR metric from 27.7 to 28.1. The effect of sentence-level ensemble is further enlarged when combined with model ensemble, which typically averages the word-level output probability distributions of multiple independently trained instances with different parameter initialization. From Table 5, we can see that sentence-level ensemble contributes more than 2% in CIDEr metric at all

model ensemble cases. Additionally, we also experimentally construct other two sentence-level ensemble models during evaluation to check the generality of this mechanism, where one is an ensemble of two Transformer(L2R) models and the other one is an ensemble of Transformer (L2R) and Transformer (R2L) models. By observing the 3rd/6th/12th/15th rows of Table 4, we can find that this mechanism can still bring non-trivial improvement on METEOR metric but at the cost of saving and running two models.

Finally, we also report the performance comparison between CBTIC model and the unidirectional Transformer model after CIDEr score optimization in Table 6. Basically, CBTIC model has a similar advantage as in the first training stage, e.g., improving the conventional Transformer(L2R) model from 127.6/22.6 to 129.8/22.8 in CIDEr/SPICE metric. And the advantage is more obvious when using better VinVL feature by improving CIDEr/SPICE metric from 134.9/23.6 to 137.5/24.2. However, we find that Transformer(R2L) model shows an undesirable phenomenon after CIDEr score optimization, i.e., generating some bad endings, e.g. ‘of a man with a soccer ball on a field’. This undermines CBTIC model to some extent and causes degradation in BLEU metrics (e.g., from 38.9 to 38.0), which focus on n-gram matching.

Metrics \ Models	CIDEr Score Optimization			
	B@4	M	C	S
Up-Down Feat.				
Transformer(L2R)	<b>38.9</b>	28.9	127.6	22.6
Transformer(R2L)	36.5	28.9	129.2	22.7
CBTIC	38.0	<b>29.1</b>	<b>129.8</b>	<b>22.8</b>
VinVL Feat.				
Transformer(L2R)	<b>41.0</b>	29.8	134.9	23.6
Transformer(R2L)	37.8	29.6	136.1	23.6
CBTIC	40.0	<b>30.1</b>	<b>137.5</b>	<b>24.2</b>

Table 6: Performance comparison with Transformer based alternatives, which have the same parameters, on MSCOCO validation set.

**How does CBTIC perform compared with state-of-the-art models?** We show the performance comparisons between our CBTIC model and state-of-the-art models on ‘Karpathy’ test split in Table 1. The performances of the single model and model ensemble are separately reported. The implementation of model ensemble follows the common practice (Rennie et al. 2017; Huang et al. 2019), which averaging the word-level output probability distributions of four independently trained instances with different parameter initialization. In general, our CBTIC model exhibits better performance than other models except for X-LAN (Pan et al. 2020) and RSTNet (Zhang et al. 2021b) in BLEU metrics in the single model setting. In the model ensemble setting, our CBTIC model outperforms all other models in all metrics, especially a large margin in CIDEr (about 5%). We think this is partly due to our CBTIC model can simultaneously take advantage of both word-level ensemble and sentence-level ensemble in ensemble setting. In addition, we also report the performance of our ensemble model on the online testing server. Table 3 details the performance over official testing images with 5 reference captions (c5) and 40 reference captions (c40). The results clearly show that our CBTIC model shows better performance across all metrics, e.g., making the absolute improvement over the best competitor RSTNet by 4.1%/4.6% in CIDEr c5/c40. It is noteworthy that we don’t list recent vision-language pre-training models (Zhou et al. 2020a; Li et al. 2020; Zhang et al. 2021a) for comparison since it’s not fair to directly compare them with non-pretraining-finetuning models.

### Qualitative Results

We showcase some qualitative results generated by our CBTIC model and conventional unidirectional Transformer model, coupled with human-annotated ground truth sentences (GT) in Figure 3. On average, CBTIC model can steal from both Transformer(l2r) and Transformer(r2l) models. For example, the CBTIC model absorbs the ‘a row of’ of Transformer (l2r) and the ‘of a building’ of Transformer (r2l) and generates a caption that is closer to ground truth in the bottom-left example. In the top-left example, CBTIC seems to directly choose the output of Trans-

former (r2l), which is the better one. We illustrate the effect of using a better feature in the 3rd column, e.g., CBTIC model fed with VinVL feature recognizes ‘surfboard’ and ‘a bar of wine bottles’. In the 4th column, we also show a kind of representative bad case of CBTIC model after CIDEr score optimization. This bad endings issue mainly derives from Transformer (r2l) ‘flow’. This is probably due to some prepositions (e.g., ‘of’) frequently follow ‘a’ in the reverse version of ground truth captions. This issue may be alleviated by using trick of removing bad endings or adding BLEU metric to the score function during self-critical training.

### CONCLUSION

In this paper, we introduce a Compact Bidirectional Transformer model for image captioning (CBTIC) that can leverage bidirectional context implicitly and explicitly while the decoder is parameter-efficient and can be executed parallelly. We conduct extensive ablation studies on MSCOCO benchmark and find that the compact architecture, which serves as a regularization for implicitly exploiting bidirectional context, and the sentence-level ensemble play more important roles than the explicit interaction mechanism. We further propose to combine word-level and sentence-level ensemble seamlessly and extend the conventional self-critical training under this architecture to achieve new state-of-the-art results in comparison with non-vision-language-pretraining models. The proposed method is orthogonal to other sophisticated methods for image captioning, including vision-language pretraining and advanced attention mechanisms, and we leave integrating these methods for better performance as our future work.

### References

- Anderson, P.; Fernando, B.; Johnson, M.; and Gould, S. 2016. Spice: Semantic propositional image caption evaluation. In *European conference on computer vision*, 382–398. Springer.
- Anderson, P.; He, X.; Buehler, C.; Teney, D.; Johnson, M.; Gould, S.; and Zhang, L. 2018. Bottom-up and top-down attention for image captioning and visual question answering. In *Proceedings of the IEEE conference on computer vision and pattern recognition*, 6077–6086.
- Ba, J. L.; Kiros, J. R.; and Hinton, G. E. 2016. Layer normalization. *arXiv preprint arXiv:1607.06450*.
- Bahdanau, D.; Cho, K.; and Bengio, Y. 2014. Neural machine translation by jointly learning to align and translate. *arXiv preprint arXiv:1409.0473*.
- Banerjee, S.; and Lavie, A. 2005. METEOR: An automatic metric for MT evaluation with improved correlation with human judgments. In *Proceedings of the acl workshop on intrinsic and extrinsic evaluation measures for machine translation and/or summarization*, 65–72.
- Caruana, R. 1997. Multitask learning. *Machine learning*, 28(1): 41–75.
- Chen, X.; Fang, H.; Lin, T.-Y.; Vedantam, R.; Gupta, S.; Dollár, P.; and Zitnick, C. L. 2015. Microsoft coco captions: Data collection and evaluation server. *arXiv preprint arXiv:1504.00325*.

- Chen, Y.-C.; Gan, Z.; Cheng, Y.; Liu, J.; and Liu, J. 2020. Distilling Knowledge Learned in BERT for Text Generation. In *Proceedings of the 58th Annual Meeting of the Association for Computational Linguistics*, 7893–7905.
- Cornia, M.; Stefanini, M.; Baraldi, L.; and Cucchiara, R. 2020. Meshed-memory transformer for image captioning. In *Proceedings of the IEEE/CVF Conference on Computer Vision and Pattern Recognition*, 10578–10587.
- Deshpande, A.; Aneja, J.; Wang, L.; Schwing, A. G.; and Forsyth, D. 2019. Fast, diverse and accurate image captioning guided by part-of-speech. In *Proceedings of the IEEE/CVF Conference on Computer Vision and Pattern Recognition*, 10695–10704.
- Devlin, J.; Chang, M.-W.; Lee, K.; and Toutanova, K. 2018. Bert: Pre-training of deep bidirectional transformers for language understanding. *arXiv preprint arXiv:1810.04805*.
- Elliott, D.; Frank, S.; and Hasler, E. 2015. Multilingual image description with neural sequence models. *arXiv preprint arXiv:1510.04709*.
- Gu, J.; Wang, G.; Cai, J.; and Chen, T. 2017. An empirical study of language cnn for image captioning. In *Proceedings of the IEEE International Conference on Computer Vision*, 1222–1231.
- He, K.; Zhang, X.; Ren, S.; and Sun, J. 2016. Deep residual learning for image recognition. In *Proceedings of the IEEE conference on computer vision and pattern recognition*, 770–778.
- Hou, J.; Wu, X.; Zhao, W.; Luo, J.; and Jia, Y. 2019. Joint syntax representation learning and visual cue translation for video captioning. In *Proceedings of the IEEE/CVF International Conference on Computer Vision*, 8918–8927.
- Huang, L.; Wang, W.; Chen, J.; and Wei, X.-Y. 2019. Attention on attention for image captioning. In *Proceedings of the IEEE/CVF International Conference on Computer Vision*, 4634–4643.
- Ji, J.; Luo, Y.; Sun, X.; Chen, F.; Luo, G.; Wu, Y.; Gao, Y.; and Ji, R. 2021. Improving image captioning by leveraging intra-and inter-layer global representation in transformer network. In *Proceedings of the AAAI Conference on Artificial Intelligence*, volume 35, 1655–1663.
- Jiang, H.; Misra, I.; Rohrbach, M.; Learned-Miller, E.; and Chen, X. 2020. In defense of grid features for visual question answering. In *Proceedings of the IEEE/CVF Conference on Computer Vision and Pattern Recognition*, 10267–10276.
- Jiang, W.; Ma, L.; Jiang, Y.-G.; Liu, W.; and Zhang, T. 2018. Recurrent fusion network for image captioning. In *Proceedings of the European Conference on Computer Vision (ECCV)*, 499–515.
- Karpathy, A.; and Fei-Fei, L. 2015. Deep visual-semantic alignments for generating image descriptions. In *Proceedings of the IEEE conference on computer vision and pattern recognition*, 3128–3137.
- Li, G.; Zhu, L.; Liu, P.; and Yang, Y. 2019. Entangled transformer for image captioning. In *Proceedings of the IEEE/CVF International Conference on Computer Vision*, 8928–8937.
- Li, X.; Yin, X.; Li, C.; Zhang, P.; Hu, X.; Zhang, L.; Wang, L.; Hu, H.; Dong, L.; Wei, F.; et al. 2020. Oscar: Object-semantic aligned pre-training for vision-language tasks. In *European Conference on Computer Vision*, 121–137. Springer.
- Lin, C.-Y. 2004. Rouge: A package for automatic evaluation of summaries. In *Text summarization branches out*, 74–81.
- Luo, R. 2020. A Better Variant of Self-Critical Sequence Training. *arXiv preprint arXiv:2003.09971*.
- Pan, Y.; Yao, T.; Li, Y.; and Mei, T. 2020. X-linear attention networks for image captioning. In *Proceedings of the IEEE/CVF Conference on Computer Vision and Pattern Recognition*, 10971–10980.
- Papineni, K.; Roukos, S.; Ward, T.; and Zhu, W.-J. 2002. Bleu: a method for automatic evaluation of machine translation. In *Proceedings of the 40th annual meeting of the Association for Computational Linguistics*, 311–318.
- Qin, Y.; Du, J.; Zhang, Y.; and Lu, H. 2019. Look back and predict forward in image captioning. In *Proceedings of the IEEE/CVF Conference on Computer Vision and Pattern Recognition*, 8367–8375.
- Ren, S.; He, K.; Girshick, R.; and Sun, J. 2015. Faster r-cnn: Towards real-time object detection with region proposal networks. *Advances in neural information processing systems*, 28: 91–99.
- Rennie, S. J.; Marcheret, E.; Mroueh, Y.; Ross, J.; and Goel, V. 2017. Self-critical sequence training for image captioning. In *Proceedings of the IEEE conference on computer vision and pattern recognition*, 7008–7024.
- Sammani, F.; and Elsayed, M. 2019. Look and modify: Modification networks for image captioning. *arXiv preprint arXiv:1909.03169*.
- Sammani, F.; and Melas-Kyriazi, L. 2020. Show, edit and tell: A framework for editing image captions. In *Proceedings of the IEEE/CVF Conference on Computer Vision and Pattern Recognition*, 4808–4816.
- Song, Z.; Zhou, X.; Mao, Z.; and Tan, J. 2021. Image Captioning with Context-Aware Auxiliary Guidance. In *Proceedings of the AAAI Conference on Artificial Intelligence*, volume 35, 2584–2592.
- Sutskever, I.; Vinyals, O.; and Le, Q. V. 2014. Sequence to sequence learning with neural networks. In *Advances in neural information processing systems*, 3104–3112.
- Vaswani, A.; Shazeer, N.; Parmar, N.; Uszkoreit, J.; Jones, L.; Gomez, A. N.; Kaiser, Ł.; and Polosukhin, I. 2017. Attention is all you need. In *Advances in neural information processing systems*, 5998–6008.
- Vedantam, R.; Lawrence Zitnick, C.; and Parikh, D. 2015. Cider: Consensus-based image description evaluation. In *Proceedings of the IEEE conference on computer vision and pattern recognition*, 4566–4575.
- Vinyals, O.; Toshev, A.; Bengio, S.; and Erhan, D. 2015. Show and tell: A neural image caption generator. In *Proceedings of the IEEE conference on computer vision and pattern recognition*, 3156–3164.

- Wang, B.; Ma, L.; Zhang, W.; Jiang, W.; Wang, J.; and Liu, W. 2019a. Controllable video captioning with pos sequence guidance based on gated fusion network. In *Proceedings of the IEEE/CVF International Conference on Computer Vision*, 2641–2650.
- Wang, C.; Yang, H.; Bartz, C.; and Meinel, C. 2016. Image captioning with deep bidirectional LSTMs. In *Proceedings of the 24th ACM international conference on Multimedia*, 988–997.
- Wang, L.; Bai, Z.; Zhang, Y.; and Lu, H. 2020. Show, Recall, and Tell: Image Captioning with Recall Mechanism. In *Proceedings of the AAAI Conference on Artificial Intelligence*, volume 34, 12176–12183.
- Wang, X.; Wu, J.; Chen, J.; Li, L.; Wang, Y.-F.; and Wang, W. Y. 2019b. VateX: A large-scale, high-quality multilingual dataset for video-and-language research. In *Proceedings of the IEEE/CVF International Conference on Computer Vision*, 4581–4591.
- Xu, K.; Ba, J.; Kiros, R.; Cho, K.; Courville, A.; Salakhudinov, R.; Zemel, R.; and Bengio, Y. 2015. Show, attend and tell: Neural image caption generation with visual attention. In *International conference on machine learning*, 2048–2057. PMLR.
- Yang, X.; Tang, K.; Zhang, H.; and Cai, J. 2019. Auto-encoding scene graphs for image captioning. In *Proceedings of the IEEE/CVF Conference on Computer Vision and Pattern Recognition*, 10685–10694.
- Yao, T.; Pan, Y.; Li, Y.; and Mei, T. 2018. Exploring visual relationship for image captioning. In *Proceedings of the European conference on computer vision (ECCV)*, 684–699.
- Yao, T.; Pan, Y.; Li, Y.; and Mei, T. 2019. Hierarchy parsing for image captioning. In *Proceedings of the IEEE/CVF International Conference on Computer Vision*, 2621–2629.
- Yao, T.; Pan, Y.; Li, Y.; Qiu, Z.; and Mei, T. 2017. Boosting image captioning with attributes. In *Proceedings of the IEEE international conference on computer vision*, 4894–4902.
- Zhang, P.; Li, X.; Hu, X.; Yang, J.; Zhang, L.; Wang, L.; Choi, Y.; and Gao, J. 2021a. Vinvl: Revisiting visual representations in vision-language models. In *Proceedings of the IEEE/CVF Conference on Computer Vision and Pattern Recognition*, 5579–5588.
- Zhang, X.; Su, J.; Qin, Y.; Liu, Y.; Ji, R.; and Wang, H. 2018. Asynchronous bidirectional decoding for neural machine translation. In *Proceedings of the AAAI Conference on Artificial Intelligence*, volume 32.
- Zhang, X.; Sun, X.; Luo, Y.; Ji, J.; Zhou, Y.; Wu, Y.; Huang, F.; and Ji, R. 2021b. RSTNet: Captioning With Adaptive Attention on Visual and Non-Visual Words. In *Proceedings of the IEEE/CVF Conference on Computer Vision and Pattern Recognition*, 15465–15474.
- Zhang, Z.; Qi, Z.; Yuan, C.; Shan, Y.; Li, B.; Deng, Y.; and Hu, W. 2021c. Open-book Video Captioning with Retrieve-Copy-Generate Network. In *Proceedings of the IEEE/CVF Conference on Computer Vision and Pattern Recognition*, 9837–9846.
- Zhang, Z.; Wu, S.; Liu, S.; Li, M.; Zhou, M.; and Xu, T. 2019. Regularizing neural machine translation by target-bidirectional agreement. In *Proceedings of the AAAI Conference on Artificial Intelligence*, volume 33, 443–450.
- Zhao, W.; Wang, B.; Ye, J.; Yang, M.; Zhao, Z.; Luo, R.; and Qiao, Y. 2018. A Multi-task Learning Approach for Image Captioning. In *IJCAI*, 1205–1211.
- Zhou, L.; Palangi, H.; Zhang, L.; Hu, H.; Corso, J.; and Gao, J. 2020a. Unified vision-language pre-training for image captioning and vqa. In *Proceedings of the AAAI Conference on Artificial Intelligence*, volume 34, 13041–13049.
- Zhou, L.; Zhang, J.; and Zong, C. 2019. Synchronous bidirectional neural machine translation. *Transactions of the Association for Computational Linguistics*, 7: 91–105.
- Zhou, Y.; Wang, M.; Liu, D.; Hu, Z.; and Zhang, H. 2020b. More grounded image captioning by distilling image-text matching model. In *Proceedings of the IEEE/CVF Conference on Computer Vision and Pattern Recognition*, 4777–4786.
- Zhou, Y.; Zhang, Y.; Hu, Z.; and Wang, M. 2021. Semi-Autoregressive Transformer for Image Captioning. In *Proceedings of the IEEE/CVF International Conference on Computer Vision (ICCV) Workshops*, 3139–3143.